Available online at www.sciencedirect.com

SciVerse ScienceDirect

Ceramics International 39 (2013) 7193–7197

CERAMICS INTERNATIONAL

www.elsevier.com/locate/ceramint

Luminescence properties of white-light long-lasting phosphor $Y_2O_2S:Dy^{3+}$, Mg^{2+}, Si^{4+}

Ping Huang[a], Fan Yang[a], Cai'e Cui[a,b,*], Lei Wang[a], Xing Lei[a]

[a]Physics and Optoelectronic Engineering College, Taiyuan University of Technology, Taiyuan 030024, China
[b]Observation and Control Technology Research Institute, Taiyuan University of Technology, Taiyuan 030024, China

Received 15 January 2013; received in revised form 19 February 2013; accepted 19 February 2013
Available online 27 February 2013

Abstract

A series of novel $Y_2O_2S:Dy^{3+}$, Mg^{2+}, Si^{4+} white-light long-lasting phosphors were synthesized by the solid-state reaction method. The $Y_2O_2S:Dy^{3+}$, Mg^{2+}, Si^{4+} phosphors were characterized by X-ray diffraction, photoluminescence and long-lasting phosphorescence spectra, and thermoluminescence curves. The samples doped with different concentrations of Dy^{3+} ions were composed of the pure Y_2O_2S phase. Under 357 nm UV excitation, the emission peaks at 486 nm and 577 nm were assigned to the $^4F_{9/2}\rightarrow{}^6H_{15/2}$ and $^4F_{9/2}\rightarrow{}^6H_{13/2}$ transitions of Dy^{3+} respectively. When Dy^{3+} concentration was 1%, the CIE chromaticity diagram was (0.28, 0.28), and the decay time could last for over 36 min (≥ 1 mcd/m^2).

Keywords: White-light long-lasting phosphors; Yttrium oxysulfide; Luminescence; Rare earths

1. Introduction

Long-lasting phosphors are a special kind of photoluminescent materials, which can still light up for a long time after removal of the excitation source. They are widely used in several fields such as emergency lighting, road signs, safety indication, and decorative craft. So far, the colors of developed long-lasting phosphors cover most of the region from blue to red [1–5]. However, the white-light long-lasting phosphors are still under investigation because the afterglow decay process of the different color emissions which are mixed to produce white emission is not consistent, and the luminescence properties of these phosphors cannot meet the application requirements. In those published literatures, the white-light long-lasting phosphors mainly include rare-earth Dy^{3+}-doped silicates [6–10] and aluminates [11], and rare-earth Tb^{3+}-doped yttrium oxysulfides [12–13]. However, the white-light luminescent material of Y_2O_2S host doped Dy^{3+} is not reported. $Y_2O_2S:Dy^{3+}$ phosphor may be an excellent material for the development of long-lasting phosphor due to the stable chemical and physical properties of Y_2O_2S and high luminescence efficiency of Dy^{3+} ion. In all these materials, the white long-lasting emission is achieved via the combination of different color emissions from an identical luminescence center in the same host. For $Y_2O_2S:Dy^{3+}$ phosphor, the white color is obtained by the appropriate mixing of blue light emission at 486 nm and yellow light emission at 577 nm.

In this paper, white long-lasting phosphors $Y_2O_2S:Dy^{3+}$, Mg^{2+}, Si^{4+} are prepared through the solid state reaction method and the effects of Dy^{3+} content on the crystal characteristics, luminescence properties and the afterglow performance of $Y_2O_2S:Dy^{3+}$, Mg^{2+}, Si^{4+} phosphors are discussed.

2. Experimental

The powder samples with a stoichiometric ratio of Y_2O_2S:0.5%–2% Dy^{3+}, 6% Mg^{2+}, 6% Si^{4+} were prepared by the solid-state reaction. Y_2O_3 (3 N), Dy_2O_3 (4 N), $MgCO_3$ (AR), SiO_2 (AR), and S (CP) were used as raw

*Corresponding author at: Physics and Optoelectronic Engineering College, Taiyuan University of Technology, Taiyuan 030024, China. Tel.: +86 351 4175345.
E-mail address: tytgcejy@sina.com (C. Cui).

0272-8842/$ - see front matter © 2013 Elsevier Ltd and Techna Group S.r.l. All rights reserved.
http://dx.doi.org/10.1016/j.ceramint.2013.02.064

materials, and Na_2CO_3 (AR) and $K_3PO_4 \cdot 3H_2O$ (AR) were added as flux. The molar ratio of Y_2O_3:S:Na_2CO_3:$K_3PO_4 \cdot 3H_2O$ component was 1:1.98:0.67:0.1. The raw materials and flux were thoroughly mixed and ground. The mixtures were calcined at 1000 °C for 30 min in reduced atmosphere with subsequent air cooling to get the products.

Phase identification of the samples was carried out by X-ray Power diffraction at 40 kV and 30 mA with a Shimadzu-6000 X-Ray generator with Cu Kα (λ = 0.15406 nm) radiation and the scan step was 0.02°. Excitation and emission spectra of the powder samples were measured using an F-280 fluorescence spectrophotometer with a 150 W Xe lamp as excitation source. The afterglow intensity decay curves and afterglow spectrum were measured using an F-4500 fluorescence spectrophotometer. The excitation light was switched off after the sample had been excited with 254 nm UV for 5 min. The afterglow decay curves were obtained by the brightness meter (ST-86LA). Thermoluminescence (TL) curves of the samples were measured on a model FJ-427A1TL meter with a heating rate of 1 K/s from room temperature to 673 K. The samples were excited for 10 min by 254 nm UV radiation standard lamp with a power of 6 W before measuring their TL curves and the afterglow decay curves. All the measurements were performed at room temperature except for the TL curves.

3. Results and discussion

3.1. Phase characterization

The XRD patterns of Y_2O_2S:1% Dy^{3+}, Mg^{2+}, Si^{4+} calcined at 1000 °C are shown in Fig. 1. The sample is composed of pure Y_2O_2S phase which accords with the JCPDS Card no. 24-1424. There is no other evident phase observed in XRD patterns of the sample except Y_2O_2S. It illustrates that co-doping a certain amount of Dy^{3+}, Mg^{2+}, Si^{4+} does not influence the basic crystal structure.

3.2. Luminescence spectra and CIE chromaticity diagram of samples

The excitation spectrum of Y_2O_2S:1% Dy^{3+}, Mg^{2+}, Si^{4+} by monitoring the 577 nm from the Dy^{3+} is shown in Fig. 2. The excitation spectrum consists of a series of lines in the 200–400 nm range with the strongest one at 357 nm and some other lines at 267, 330, 371, and 391 nm. The peak about 267 nm is attributed to the absorption band of the Y_2O_2S host lattice [14]. Due to the dense and overlapped nature of the excitation states in the $4f^9$ configuration of Dy^{3+} in the ultraviolet spectral range, these excitation peaks at 330 nm, 371 nm and 391 nm can only be tentatively ascribed to the transitions from the $^6H_{15/2}$ ground state to the excitation states of $^4I_{9/2}$, $^4F_{7/2}$ and $^4G_{11/2}$, respectively [15]. The excitation spectra of the other samples are similar to those in Fig. 2, so they are not shown here.

The emission spectra of samples with different concentrations of Dy^{3+} are shown in Fig. 3. All of the emissions are ascribed to the 4f–4f transitions of Dy^{3+}. Under the excitation at 357 nm, the blue emission peaking at 486 nm and yellow emission peaking at 577 nm are assigned to the $^4F_{9/2} \rightarrow {}^6H_{15/2}$ and $^4F_{9/2} \rightarrow {}^6H_{13/2}$ transitions of Dy^{3+} respectively. The white-light can be obtained by the appropriate mixing of them. The emission lines of Dy^{3+} are broadened somewhat because there are several Stark levels for the $^4F_{9/2}$ and ^6H_J levels [11]. With the increase of concentration of Dy^{3+} from 0.5% to 2.0%, lots of Y^{3+} (r=0.090 nm) ions are replaced by Dy^{3+} (r=0.091 nm) ions which act as luminescence centers, so the intensity of emission spectra is increased gradually. The sample doped with 2% Dy^{3+} has the strongest emission intensity. This indicates that concentration quenching has not occured when the content of Dy^{3+} reaches 2%.

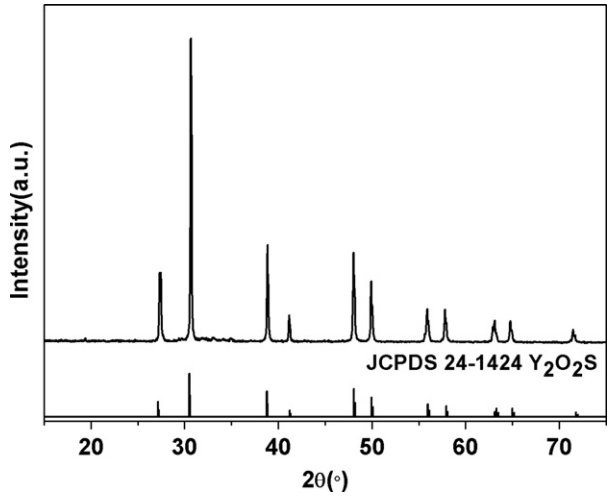

Fig. 1. The XRD patterns of Y_2O_2S:1% Dy^{3+}, Mg^{2+}, Si^{4+} phosphor and JCPDS Cards no. 24-1424.

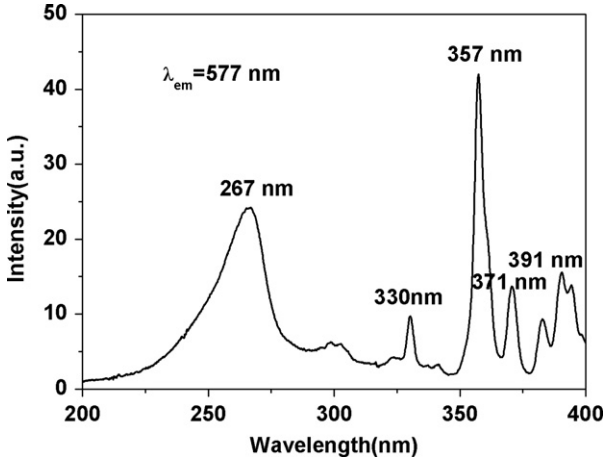

Fig. 2. The excitation spectrum of Y_2O_2S:1% Dy^{3+}, Mg^{2+}, Si^{4+} phosphor.

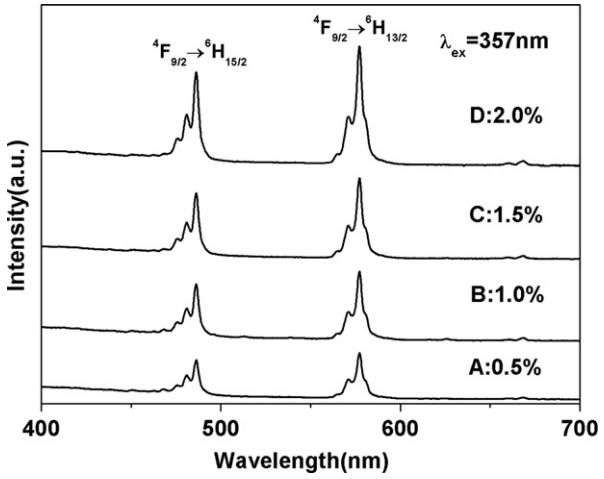

Fig. 3. The emission spectra of $Y_2O_2S:Dy^{3+}$, Mg^{2+}, Si^{4+} phosphors with different concentrations of Dy^{3+}.

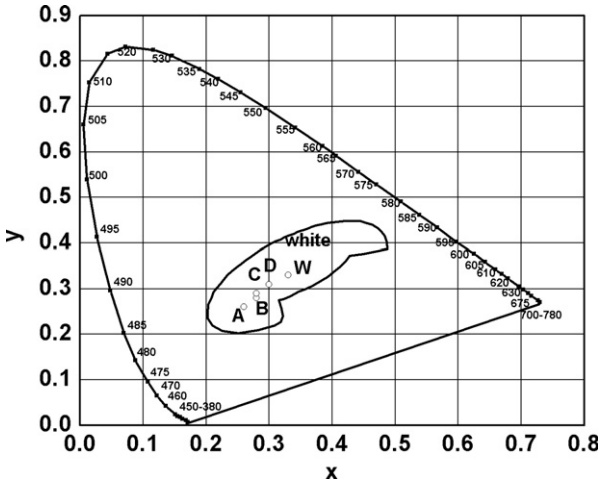

Fig. 4. The CIE chromaticity diagram of $Y_2O_2S:Dy^{3+}$, Mg^{2+}, Si^{4+} phosphors with different concentrations of Dy^{3+}: (a) 0.5%; (b) 1%; (c) 1.5%; and (d) 2%.

The CIE chromaticity diagram of $Y_2O_2S:Dy^{3+}$, Mg^{2+}, Si^{4+} with different concentrations of Dy^{3+} is shown in Fig. 4. The CIE chromaticity coordinates of samples can be obtained by the emission spectra. They vary systematically from (0.26, 0.26), (0.28, 0.28), (0.28, 0.29) to (0.30, 0.31) corresponding to points A, B, C and D. It is because the intensity of yellow emission is increased gradually with the increase of concentration of Dy^{3+}. This change is consistent with Fig. 3. In Fig. 4, point D is the closest to point W (0.33, 0.33) which delegates the ideal white. Even so, all points locate at the white-light region.

The afterglow intensity decay curves and the afterglow spectra of Y_2O_2S:1% Dy^{3+}, Mg^{2+}, Si^{4+} phosphor after irradiation with 254 nm UV radiation for 5 min are shown in Fig. 5. The decay curves of 486 nm and 577 nm emissions which originate from the same luminescence center are similar. This indicates that the emissions have similar decay ratio. From the inset picture of Figs. 5 and 3,

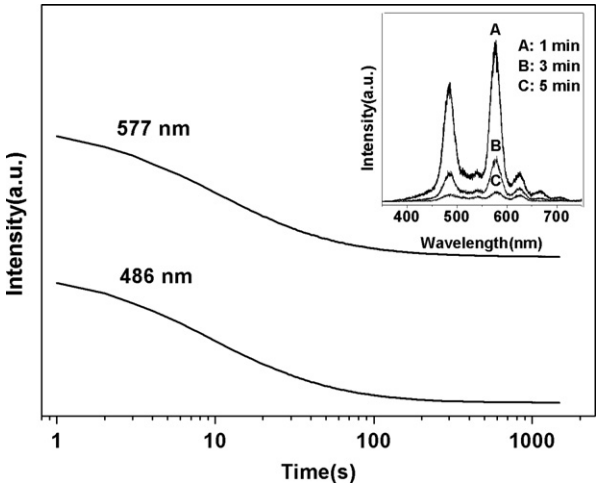

Fig. 5. The afterglow intensity decay curves of different emissions in Y_2O_2S:1% Dy^{3+}, Mg^{2+}, Si^{4+} phosphor (the inset picture shows the afterglow spectra of the sample after the excitation source is switched off at different times).

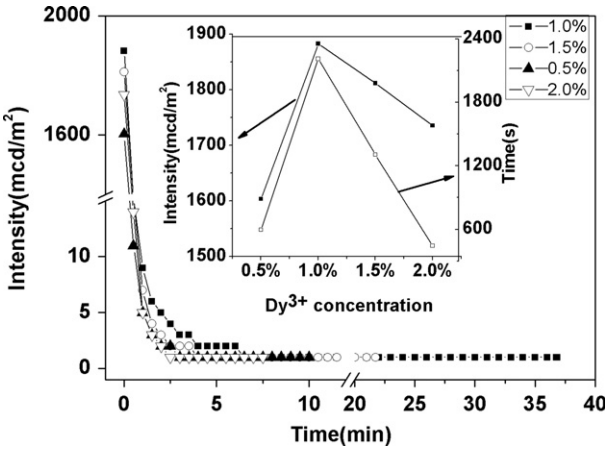

Fig. 6. The afterglow decay curves of $Y_2O_2S:Dy^{3+}$, Mg^{2+}, Si^{4+} phosphors with different concentrations of Dy^{3+} (the inset picture shows the initial intensity and afterglow time with different concentrations of Dy^{3+}).

the afterglow spectra are observed in the same region as the emission spectra, and the shape and location of main emission peaks of the afterglow spectra and the emission spectra are found to be almost identical. Thereby, a stable white emission in the sample can be produced during the decay process.

3.3. Afterglow decay curves and TL curves of samples

The afterglow decay curves of samples with different concentrations of Dy^{3+} are shown in Fig. 6. The sample doped with 1% Dy^{3+} shows the optimal initial luminance and afterglow time, and the decay time can last for over 36 min (≥ 1 mcd/m^2). It is reported that the decay behavior of long lasting phosphors can be calculated by fitting

the decay data using the following equation [16]:

$$I = A_1\exp(-t/\tau_1)+A_2\exp(-t/\tau_2) \quad (1)$$

where I is the phosphorescence intensity; A_1 and A_2 are constants; t is the time; and τ_1 and τ_2 are the decay times for the exponential components. Using the software Origin 8.0, the parameters of the samples can be obtained, which are listed in Table 1. The values of τ_2 are bigger than those of τ_1, which implies that the decay processes of phosphors are fitted by initial rapid decay and then a stable decay. The afterglow mechanisms can be explained by the contribution from the electron traps formed by the co-doped Mg^{2+} and Si^{4+} ions. They occupy the same lattice sites as Y^{3+} ions do. To keep charge balance, $2Y^{3+}$ ions are replaced by $1Mg^{2+}$ and $1Si^{4+}$ ion. However, such replacement breaks the charge balance around local lattice site and causes the formation of new electronic donating and accepting levels between the host lattice band gap, that is, an excessive positive charge which serves as the electron trap around the doped Si^{4+} ion is created. One of the ions absorbs energy and thermally transfers the excited electrons to another ion which serves as trap centers. The trap of stored energy which is constituted by Mg^{2+} and Si^{4+} ions serves as the donor leveling, and Dy^{3+} serves as the acceptor leveling. The trapping of excited electrons and thermally released processes cause the appearance of afterglow [17].

TL curve is an important tool to investigate the luminous properties of phosphor. The afterglow luminance and time are found to depend strongly on the depth and the density of traps [18,19]. Fig. 7 represents the TL curves of samples with different concentrations of Dy^{3+}. For all the samples, the TL peaks are located in the region of 323–383 K which are helpful to produce a longer duration of afterglow [20]. With the increase of content of Dy^{3+} ions, the intensity of TL peak is increased gradually, and the intensity of TL peak reaches maximum when the concentration of Dy^{3+} ions is 1%. When the concentration of Dy^{3+} ions exceeds 1%, the intensity of TL peak begins to decrease. This is possible due to the retrapping probability which is larger with higher concentration of Dy^{3+} [6]. The depth of traps in the samples can be estimated by analyzing the TL peak using equations given by Chen [21].

$$E = c_\tau k T_m^2/\tau - b_\tau 2kT_m \quad (2)$$

Table 1
Fitting parameters of samples.

Concentration of Dy^{3+} (mol)	Parameters	
	τ_1/s	τ_2/s
0.5%	5.06	33.61
1.0%	6.99	62.89
1.5%	5.46	35.93
2.0%	5.02	30.85

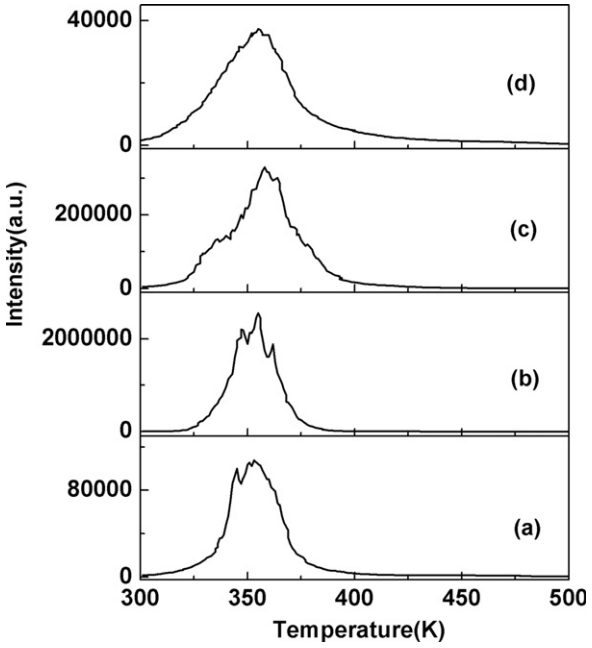

Fig. 7. The TL curves of Y_2O_2S:Dy^{3+}, Mg^{2+}, Si^{4+} phosphors with different concentrations of Dy^{3+}: (a) 0.5%; (b) 1%; (c) 1.5%; and (d) 2.0%.

Table 2
E values of the samples with different concentrations of Dy^{3+}.

Concentration of Dy^{3+} (mol)	T_m (K)	T_1 (K)	T_2 (K)	τ (K)	δ (K)	ω (K)	μ_g	E (eV)
0.5%	341	353	367	12	14	26	0.54	1.54
1.0%	342	353	365	11	12	23	0.52	1.65
1.5%	345	358	372	13	14	27	0.52	1.41
2.0%	335	355	371	20	16	36	0.44	0.76

$$c_\tau = 1.51+3(\mu_g-0.42), \quad b_\tau = 1.58+4.2(\mu_g-0.42) \quad (3)$$

$$\tau = T_m-T_1, \quad \delta = T_2-T_m, \quad \omega = T_2-T_1, \quad \mu_g = \delta/\omega \quad (4)$$

where T_m is the peak temperature, T_1 and T_2 are the low and high temperatures corresponding to the half peak intensity, τ is the left half width, δ is the right half width, ω is the total half intensity width, k is Boltzmann's constant, and μ_g is the symmetry factor. The trap parameters are calculated using Eqs. (2–4) and listed in Table 2.

In order to produce long phosphorescence, the trapping levels need to locate at a suitable depth. If the trap level is too shallow, only small amount of electrons can be captured to traps. Under the action of thermal disturbances, electrons are easily released from traps and then combined with holes in the ground state, which results in shorter afterglow time. On the other hand, if the trap level is too deep, it is hard to return electrons to the excited state levels at room temperature, which also results in poor afterglow property. The sample doped with 1% Dy^{3+} has the deepest trap depth, and it shows the optimal initial

luminance and afterglow time. From Fig. 7 and Table 2, for the $Y_2O_2S:Dy^{3+}$, Mg^{2+}, Si^{4+} phosphor, the high trap density and deep trap depth is suitable to produce optimal afterglow properties.

4. Conclusions

The novel white-light long-lasting phosphors $Y_2O_2S:Dy^{3+}$, Mg^{2+}, Si^{4+} with different concentrations of Dy^{3+} were prepared at 1000 °C for 30 min in reduced atmosphere through the solid state reaction method. Under 357 nm UV irradiation, the white-light could be obtained by the appropriate mixing of blue emission at 486 nm and yellow emission at 577 nm of Dy^{3+}. The sample doped with 1% Dy^{3+} had the highest trap density and the deepest trap depth which led to the optimal initial luminance and afterglow time. Therefore, for the white long-lasting phosphor $Y_2O_2S:Dy^{3+}$, Mg^{2+}, Si^{4+}, the optimal concentration of Dy^{3+} doped is 1%.

Acknowledgments

This present work was financially supported by the National Natural Science Foundation of China (No. 51072128), the Key Research Project of Science and Technology of Shanxi (No. 2011 0321040-01) and the Program for the Top Young Academic Leaders of Higher Learning Institutions of Shanxi.

References

[1] T. Matsuzawa, Y. Aoki, N. Takeuchi, Y. Murayama, A new long phosphorescent phosphor with high brightness $SrAl_2O_4:Eu^{2+}$, Dy^{3+}, Journal of the Electrochemical Society 143 (1996) 2670–2673.

[2] S.Y. Kaya, E. Karacaoglu, B. Karasu, Effect of Al/Sr ratio on the luminescence properties of $SrAl_2O_4:Eu^{2+}$, Dy^{3+} phosphors, Ceramics International 38 (2012) 3701–3706.

[3] H.H. Zeng, X.M. Zhou, L. Zhang, X.P. Dong, Synthesis and luminescence properties of a novel red long lasting phosphor $Y_2O_2S:Eu^{3+}$, Si^{4+}, Zn^2, Journal of Alloys and Compounds 460 (2008) 704–707.

[4] P. Huang, Q.C. Zhang, C. Cui, J. Li, Influence of excitation wavelengths on luminescent properties of $Sr_3Al_2O_6:Eu^{2+}$, Dy^{3+} phosphors prepared by sol–gel-combustion processing, Optical Materials 33 (2011) 1252–1257.

[5] G.H. Kim, S.J. Lee, Y.J. Kim, The effects of zinc on the structural and luminescent properties of $Ca_{1-x}Zn_xTiO_3:Pr^{3+}$ phosphors, Optical Materials 34 (2012) 1860–1864.

[6] Y.L. Liu, B.F. Lei, C.S. Shi, Luminescent properties of a white afterglow phosphor $CdSiO_3:Dy^{3+}$, Chemistry of Materials 17 (2005) 2108–2113.

[7] J.Y. Kuang, Y.L. Liu, J.X. Zhang, White-light-emitting long-lasting phosphorescence in Dy^{3+}-doped $SrSiO_3$, Journal of Solid State Chemistry 179 (2006) 266–269.

[8] Y.H. Chen, X.R. Cheng, Z.M. Qi, M. Liu, C.S. Shi, Comparison study of the luminescent properties of the white-long afterglow phosphors $Ca_xMgSi_2O_{5+x}:Dy^{3+}$($x=1$, 2, 3), Journal of Luminiscence 129 (2009) 531–535.

[9] B. Liu, L. Kong, C. Shi, White-light long-lasting phosphor $Sr_2MgSi_2O_7:Dy^{3+}$, Journal of Luminiscence 122–123 (2007) 121–124.

[10] Y. Gong, Y.H. Wang, Y.Q. Li, X.H. Xu, Ce^{3+}, Dy^{3+} co-doped white-light long-lasting phosphor $Sr_2Al_2SiO_7$ through energy transfer, Journal of the Electrochemical Society 6 (2010) J208–J211.

[11] B. Liu, C.S. Shi, Z.M. Qi, Potential white-light long-lasting phosphor Dy^{3+}-doped aluminate, Applied Physisc Letters 86 (2005) 191111.

[12] B. Liu, C.S. Shi, Z.M. Qi, White-light long-lasting phosphorescence from Tb^{3+}-activated Y_2O_2S phosphor, Journal of Physics and Chemistry of Solids 67 (2006) 1674–1677.

[13] L. Lin, K. Chen, Z.F. Wang, B.G. You, Y.H. Chen, W.P. Zhang, C.S. Shi, A white long lasting phosphor $Y_2O_2S:Tb^{3+}$, Sm^{3+}: an improvement of $Y_2O_2S:Tb^{3+}$, Journal of Rare Earths 26 (2008) 648–651.

[14] Z.L. Wang, Y.H. Wang, J.C. Zhang, Y.H. Lu, The photoluminescence properties of Eu^{3+}, Bi^{3+} co-doped yttrium oxysulfide phosphor under vacuum ultraviolet excitation, Materials Research Bulletin 44 (2009) 1183–1187.

[15] A. Elizebeth, V. Thomas, G. Jose, G. Jose, N.V. Unnikrishnan, C. Joseph, M.A. Ittyachen, Crystal Research and Technology 39 (2004) 105–110.

[16] B.F. Lei, B. Li, H.R. Zhang, W.L. Li, Preparation and luminescence properties of $CaSnO_3:Sm^{3+}$ phosphor emitting in the reddish orange region, Optical Materials 29 (2007) 1491–1494.

[17] P.F. Ai, W.Y. Li, L.Y. Xiao, Y.D. Li, H.J. Wang, Y.L. Liu, Monodisperse nanospheres of yttrium oxysulfide: synthesis, characterization, and luminescent properties, Ceramics International 36 (2010) 2169–2174.

[18] T. Aitasalo, P. Dereń, J. Hölsä, H. Jungner, J.C. Krupa, M. Lastusaari, J. Legendziewicz, J. Niittykoski, W. Stręk, Persistent luminescence phenomena in materials doped with rare earth ions, Journal of Solid State Chemistry 171 (2003) 114–122.

[19] L. Jing, C.K. Chang, D.L. Mao, B. Zhang, A new long persistent blue-emitting $Sr_2ZnSi_2O_7:Eu^{2+}$, Dy^{3+} prepared by sol–gel method, Materials Letters 58 (2004) 1825–1829.

[20] P.F. Ai, Y.L. Liu, L.Y. Xiao, H.J. Wang, J.X. Meng, Synthesis of $Y_2O_2S:Eu^{3+}$, Mg^{2+}, Ti^{4+} hollow microspheres via homogeneous precipitation route, Science and Technology of Advanced Materials 11 (2010) 035002 (5 pp).

[21] R. Chen, Glow curves with general order kinetics, Journal of the Electrochemical Society: Solid State Science and Technology 116 (1969) 1254–1257.